sustainability

MDPI

Article

Removal Efficiency and Adsorption Kinetics of Methyl Orange from Wastewater by Commercial Activated Carbon

Gabriel Valentin Serban †, Vasile Ion Iancu *, Cristina Dinu, Anda Tenea, Nicoleta Vasilache, Ionut Cristea, Marcela Niculescu, Ioana Ionescu and Florentina Laura Chiriac †

National Research and Development Institute for Industrial Ecology—ECOIND, Drumul Podu Dambovitei Street 57–73, 060652 Bucharest, Romania; gabriel.serban@ecoind.ro (G.V.S.); cristina.dinu@incdecoind.ro (C.D.); anda.tenea@incdecoind.ro (A.T.); nicoleta.vasilache@incdecoind.ro (N.V.); ionut.cristea@incdecoind.ro (I.C.); marcela.niculescu@incdecoind.ro (M.N.); ioana.ionescu@incdecoind.ro (I.I.); laura.chiriac@incdecoind.ro (F.L.C.)

* Correspondence: vasile.iancu@incdecoind.ro

† These authors contributed equally to this work.

Abstract: This research investigates commercial activated carbon (AC) potential to remove methyl orange (MO) dye removal from aqueous solution using a batch process. The AC material was characterized using FTIR spectroscopy and SEM analysis. The effect of the main operating parameters, such as the pH, adsorbent dosage, contact time, and initial dye concentration, was studied. MO removal could be accomplished within 30 min at a pH value of 3. The calculated maximum MO adsorption capacity onto activated carbon was 129.3 mg/g, while the removal efficiency was 97.8%. Adsorption results were analyzed by studying the Langmuir and Freundlich isotherm models. The MO adsorption data on activated carbon were better explained by the Langmuir isotherm than by the Freundlich isotherm. The pseudo-second-order kinetic model may have had an effect on the MO dye adsorption on AC material. This research showed that the commercial activated carbon can be used as an effective sorbent for MO removal from wastewater sample. Moreover, the AC material has good reusability and practical utilization capacities.

Keywords: activated carbon; methyl orange; adsorption isotherm; kinetics models; wastewater

Citation: Serban, G.V.; Iancu, V.I.; Dinu, C.; Tenea, A.; Vasilache, N.; Cristea, I.; Niculescu, M.; Ionescu, I.; Chiriac, F.L. Removal Efficiency and Adsorption Kinetics of Methyl Orange from Wastewater by Commercial Activated Carbon. *Sustainability* **2023**, *15*, 12939. https://doi.org/10.3390/su151712939

Academic Editor: Andreas Angelakis

Received: 2 July 2023
Revised: 11 August 2023
Accepted: 23 August 2023
Published: 28 August 2023

1. Introduction

The discharge of vast quantities of organic contaminants into the environment is a major concern globally [1]. Synthetic dyes are a class of contaminants that must be removed from wastewater before being discharged into aquatic ecosystems due to their toxicity and negative repercussions on photosynthetic activity [2,3]. Once in natural bodies of water, dyes lead to an increase in color saturation, thus preventing the penetration of sunlight into the water, and thereby endangering the life of aquatic organisms [4].

Different industries, mainly paper, printings, textiles and leather, but also food processing, cosmetics, and pharmaceuticals, release high amounts of wastewater-containing dyes into water bodies, which receive the discharged effluents [5]. It is estimated that every year, more the 700,000 tons of dyes are disposed of worldwide [6].

One of the most common synthetic dyes is methyl orange (MO). MO is an anionic acid dye most commonly used both as a coloring pigment in the textile industry and as an indicator in laboratory experiments. Wastewater with a MO content has a low capacity for biological and/or chemical treatment. MO poses a risk to both human health and aquatic organisms as it has carcinogenic and genotoxic potential [7]. Thus, the need to develop cost-effective methods for the removal of MO and other synthetic dyes from wastewater has become a pressing concern of the scientific community in recent years.

Researchers have used different approaches over time, such as physical, chemical, or biological processes, in order to mitigate environmental metals, dyes, and other organic pollutants [8–12]. Micellar solubilization is also a widely used method for organic pollutant

removal from aqueous solution, incorporating them into or onto micelles [13–15]. Adsorption is the most common process for removing dyes from aqueous solutions [16–20]. Unlike adsorption, precipitation coagulation and electrolysis have a number of disadvantages, such as the use of chemicals, the production of toxic sludge beds, high operating costs, and corrosion [21–23]. Compared with other treatment methods, adsorption has some advantages, such as low cost, low sludge volume, easy operation, efficiency, and flexibility [24,25]. However, among the disadvantages of the adsorption process are the toxicity of the spent adsorbents and the application of chemical substances for desorption, not to mention the relocation of the contamination load more than its removal [7].

Various adsorbent materials were used to remove dye molecules from aqueous samples, such as zeolite [26], resins [16], clays [17], composite materials [14], biomass [27], and activated carbon [28,29]. Of all the adsorbents that are referred to above, activated carbon (AC) is one of the most popular materials used to remove dyes from aqueous solutions. Due to the large specific surface area as well as the well-defined porous structure, activated carbon has an excellent removal capacity for dyes, and it has the advantage of being an environmentally friendly, economic, and technically favorable method to apply to wastewater [30,31]. Recent studies have focused on obtaining low-cost adsorbents, producing activated carbon using cheap and readily available materials, such as date stones [32], longan seed-activated carbon [33], Prosopis juliflora bark [34], orange/citrus peels-activated carbon [35], populous leaf charcoal [36], etc.

The same material was tested in order to remove some pharmaceutical compounds from wastewater [37], and the results showed that the maximum adsorption capacities of the AC material ranged from 0.64 to 0.85 mg/g. Considering that pharmaceutical residues are not the only organic contaminants of wastewater, we followed the testing of the same adsorbent material for the removal of synthetic dyes from aqueous solutions, choosing methyl orange dye as a representative of this class of pollutants.

In this context, the aim of this research had six objectives: (1) to optimize the MO adsorption conditions (pH, MO concentration, adsorbent dosage, and contact time); (2) to fit the equilibrium experimental results using Langmuir and Freundlich adsorption isotherm models; (3) to study the kinetic process of the MO adsorption (pseudo-first-order, pseudo-second-order, and intra-particle diffusion); (4) to determine thermodynamic parameters of the adsorption process; (5) to apply optimized adsorption conditions in order to remove MO from real wastewater samples; and (6) to determine desorption characteristics and reusability of the commercial AC. Compared to other studies, this work reports a simple, fast, eco-friendly, and efficient method for MO removal from aqueous solutions using commercial activated carbon, with good results in wastewater treatment and reusability (up to five cycles). The results of this study can contribute to the development of competency and sustainable methods for the treatment of wastewater containing MO, thereby reducing its environmental impact.

2. Materials and Methods

2.1. Chemicals and Reagents

Methyl Orange dye (purity > 95%) was purchased from Sigma-Aldrich (Darmstadt, Germany). The activated carbon was acquired from Trace Elemental Instruments (Delft, The Netherlands) with the following characteristics: 10–50 µm particle size, 256 m^2/g specific surface area, 14.7 Å pore size, and 870 m^2/g total pore area. Acetonitrile (HPLC grade), methanol (HPLC grade), ammonium acetate (≥98%), sodium hydroxide (≥99%), and hydrochloric acid (37%) were purchased from Merck (Darmstadt, Germany). The basic standard solution, with a concentration of 1000 mg/L, was prepared in methanol. The stock solution was diluted using ultra purified water to the precise concentrations reacquired.

2.2. Characterization of Commercial AC

FTIR spectra of the commercial activated carbon was acquired between the 4400 and 400 cm^{-1} using a FTIR Spectrum BX II Perkin Elmer spectrophotometer (Waltham, MA,

USA). An SEM study of the adsorbent material was obtained using a piece of Quanta 250 FEG equipment, which was acquired from Thermo Fisher Scientific (Waltham, MA, USA).

2.3. Adsorption Studies

The MO adsorption mechanism on AC was studied using the batch method. All of the experiments were effectuated under stirring (150 rpm) and at a constant temperature of 25 ± 1 °C in 250 mL Erlenmeyer stoppered flasks. The initial MO solution involved had a concentration of 10 mg/L. Thus, volumes of MO solution of 50 mL were contacted with amounts of 0.005 g of activated carbon. Samples were collected at well-established time intervals. The supernatant was centrifuged at 5000 rpm for 5 min, and the MO concentration was analyzed using the HPLC technique. To establish the optimum conditions and to obtain the highest adsorption capacity, the effects of the operational parameters were evaluated: dosage effect (0.001–0.010 g AC), interaction time (1–120 min), MO concentration (5–100 mg/L MO), and pH (3–11, using HCl and KOH solutions of different concentrations).

The MO removal rate (% R) at time t, the adsorption capacity, Q_t (mg/g) at time t and the adsorption capacity at equilibrium, Q_e (mg/g), and the distribution coefficient, kd, are described by Equations (1)–(4):

$$\% R = (C_0 - C_t)/C_0 \times 100 \quad (1)$$

$$Q_t = (C_0 - C_{t)} \times V)/m \quad (2)$$

$$Q_e = (C_0 - C_e) \times V)/m \quad (3)$$

$$Kd = [(C_0 - Q_e) \times m]/(C_e \times V) \quad (4)$$

where C_0 is the initial concentration of MO in the solution (mg/L); C_t is the MO concentration at time t (mg/L); C_e is the MO concentration at equilibrium; Q_t is the adsorption capacity at time t (mg MO/g); Q_e is the adsorption capacity at equilibrium (mg/g); V is the volume of the solution (L); and m is the amount of adsorbent material used (g).

2.4. pH_{pzc}

The point of zero charge (pH_{pzc}) was evaluated from acid-base titration. Different flasks containing 50 mL of 0.01 M NaCl solution were prepared. The pH was adjusted from 2 to 12 using 0.01 M NaOH or HCl. In each flask, 0.10 g of AC was added, and was then sealed and shacked for 24 h. Blank tests without AC sample were also prepared.

2.5. Adsorption Isotherms

The adsorption isotherm represents the non-kinetic correlation between the adsorption capacity at equilibrium (Q_e) and the MO concentration at equilibrium (C_e). The adsorption isotherms were determined for 5 mg of AC by varying the MO concentration between 5 and 100 mg/L (5, 10, 25, 50, 75 and 100 mg/L). The flasks containing 50 mL solution were stirred for 30 min (at 150 rpm) at pH = 3. Two models were modeled using linear regression by the Excel 2019 software. Equations (5) and (7) present the Langmuir and Freundlich equations, respectively, while Equation (6) describes the separation factor of the adsorption process [38,39]:

$$Q_e = (Q_m \times K_L \times C_e)/(1 + K_L \times C_e) \quad (5)$$

$$R_L = 1/(1 + C_0 \times K_L) \quad (6)$$

$$Q_e = K_F C_e^{1/n} \quad (7)$$

where C_e (mg/L) is the MO equilibrium concentration; Q_m (mg/g) is the maximum monolayer adsorption capacity; K_L (L/mg) is the Langmuir equilibrium constant; and R_L is

the separation factor. The R_L shows that the isotherm is favorable ($0 < R_L < 1$), unfavorable ($R_L > 1$), linear ($R_L = 1$), or irreversible ($R_L = 0$). K_F and n are Freundlich constants, and 1/n is the heterogeneity factor (n > 1 represent favorable adsorption).

2.6. Adsorption Kinetics

Kinetic studies provide details on the characteristics of the adsorption process. The MO adsorption on AC was studied using 5 mg of AC and 50 mL of the 10 mg/L MO. The mixture was shaken at 150 rpm and at room temperature between 5 and 30 min at a pH of 3. The MO concentration at the different contact times was determined using the HPLC technique. The pseudo-first and pseudo-second-order kinetic as well as the intra-particle diffusion models were used to evaluate the adsorption process of MO on AC [40] based on Equations (8)–(10), respectively:

$$\mathrm{Ln}\,(Q_e - Q_t) = \mathrm{Ln}Q_e - k_1 \quad (8)$$

$$t/Q_t = 1/(k_2 \times Q_e^2) + 1/Q_e \quad (9)$$

$$Q_t = k_{id} \times t^{1/2} + C_{id} \quad (10)$$

where k_1 (min^{-1}) is the pseudo-first-order kinetic rate constant, k_2 (g/(mg × min)) is the rate constant of pseudo-second-order kinetic model, k_{id} is the intra-particle diffusion rate constant (mg/g $min^{1/2}$), and C_{id} is the intra-particle diffusion constant.

2.7. Thermodynamic Study

Thermodynamic parameters, namely, Gibbs free energy (ΔG°), enthalpy (ΔH°), and entropy (ΔS°), are typically used to describe the adsorption process. The thermodynamic parameters were calculated using the following equations:

$$\Delta G^\circ = -RT\,\mathrm{Ln}\,K_L{}^\circ \quad (11)$$

$$\mathrm{Ln}\,K_L{}^\circ = (\Delta S^\circ/R) - (\Delta H^\circ/RT) \quad (12)$$

$$K_L{}^\circ = K_L(L/mg) \times 1000\,(mg/g) \times M\,(g/mol) \times C^\circ\,(mol/L) \quad (13)$$

$$\Delta G^\circ = \Delta H^\circ - T\Delta S^\circ \quad (14)$$

where R = 8.314 J/mol K is the universal gas constant, T is the absolute temperature (K), K_L is the Langmuir constant, 1000 is the factor that converts g to mg, M is the molar mass of MO (327.33 g/mol), and C° = 1 mol/L.

ΔH° and ΔS° parameters were estimated from the slope and the intercept of the plot Ln $K_L{}^\circ$ vs. 1/T. ΔG° (kJ/mol) values were recalculated after the ΔH° and ΔS° were estimated.

2.8. Instrumental Analysis

Analytical experiments were performed using an Agilent 1200 HPLC (Agilent Technologies, Santa Clara, CA, USA) system with DAD detection. An Acclaim Surfactant Plus chromatographic column (15 cm × 3 mm × 3 µm) kept at 30 °C was used to determine the MO concentration. The mobile phase composition consisted of 100 mM ammonium acetate at a pH of 5.0 (A) and acetonitrile (B) in an isocratic mode (50/50). The flow rate of the mobile phase was 0.5 mL/min, the injection volume was 10 µL, and the chromatographic run time was 10 min. MO detection was performed at 425 nm.

2.9. Quality Assurance and Quality Control

All experiments were performed in triplicate. For each set of samples, a blank sample and an analytical standard solution were injected for control. The DAD response proved to be linear over the entire concentration range (0.1–100 mg/L), with a correlation coefficient

of 0.9999. The RSD values obtained from the experiments showing the intra-day and inter-day precision were 3.27 and 7.82%, respectively, while the limit of quantitation (LOQ) was 0.1 mg/L.

3. Results and Discussion

3.1. Chemical and Physical Characterization of the Adsorbent Material

Figure 1 shows the FTIR spectra of the commercial activated carbon. The broad bands that are situated in the region 3720.53–3739.49 cm^{-1} are attributed to the hydroxyl (–OH) groups, while the peaks that are situated in the range of 2850.43–2918.89 cm^{-1} are related to the C-H stretching vibrations of the methyl groups. The peak situated at 1534.63 cm^{-1} can be associated to C=C stretching vibration. The bands at 2258.10, 2334.60, and 2352.63 cm^{-1} are characteristic of the C≡C stretching vibration.

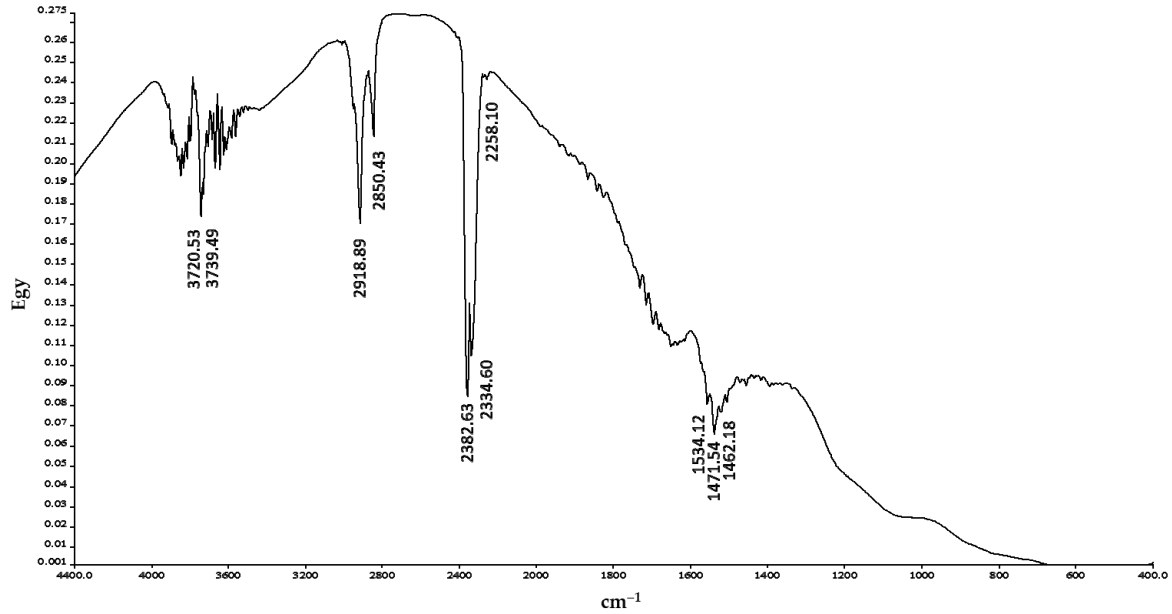

Figure 1. FTIR spectra of the commercial AC.

The SEM image shows that the surface morphology of the commercial activated carbon is composed of small-sized carbon pieces that are uniformly distributed (Figure 2). This structure involves both a large number of pores and a high probability that the MO will be adsorbed in these pores. The macropores are easily observable, making the diffusion of a great number of MO molecules into the pores and the adsorption of the MO molecules on the AC surface easy.

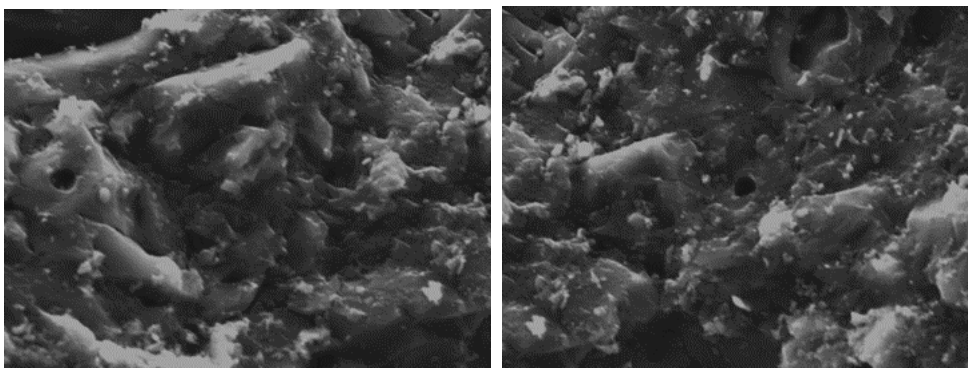

Figure 2. SEM image of the commercial AC recorded at scale 10 μm.

3.2. Adsorption Study

In order to avoid the excessive use of the adsorbent material, the evaluation of the adsorbent dosage is an important parameter in the study of the adsorption process [41]. The absorbent dose could influence the performance and the adsorption capacity of the adsorbent material. The data obtained after using different amounts of adsorbent material are presented in Figure 3a. The removal percentage of MO increased from 35% to 93% when the amount of AC increased from 0.001 g to 0.01 g. Increasing the dose of AC implies a larger number of active sites for the interaction between MO and AC. Thus, with the increase in the specific surface area, the percentage of MO that was removed also increased. The MO removal process worked satisfactorily using low doses of AC, which means that this adsorbent material has enough active sites on the surface for MO to adsorb efficiently. For the range 0.007–0.01 g AC, a flattening of the graph was observed, which indicates that the specific surface area of AC in the aqueous solution was greater than the number of MO molecules, and many active sites thereby remain unused, which decreases the adsorption capacity [42].

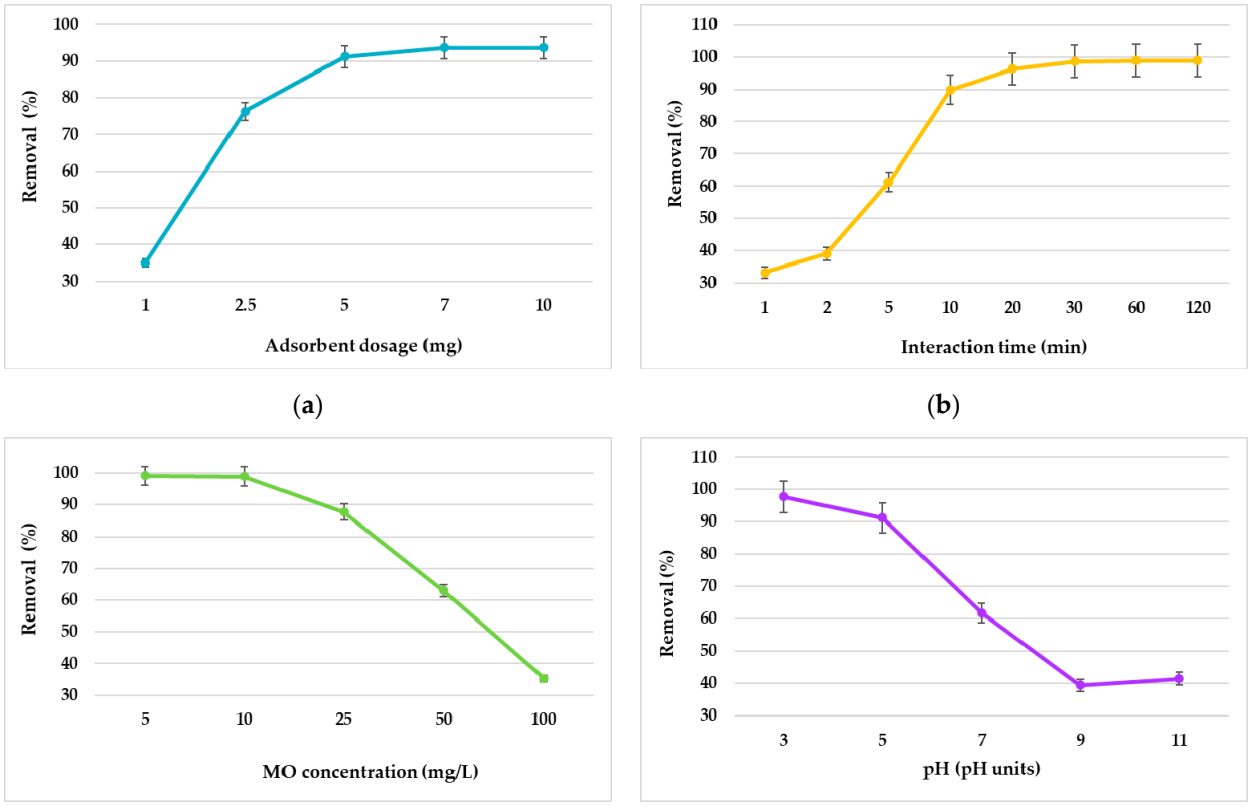

Figure 3. Effect of (**a**) adsorbent dosage, (**b**) interaction time, (**c**) MO concentration, and (**d**) pH on the MO adsorption by the AC.

The experimental results show that MO removal by adsorption on AC was a fast process (Figure 3b), and this is supported by the reduced value of the time required to reach the equilibrium, which was approximately 30 min of contact between the MO and the AC. The equilibrium was achieved in two stages. The first stage was a fast stage (from 0 to 20 min), observing a sudden increase in the MO removal by adsorption on AC. This sudden variation was due to the large number of free active sites on the activated carbon surface that are available for MO molecules. The second stage was a slower stage. This slow growth was determined by the reduced number of free active sites on the carbon surface, as

some of them have already been occupied by MO molecules. Thus, the adsorbent reaches the saturation point after 30 min.

The initial MO concentration is an important parameter that has an effect on adsorption performance and capacity. Establishing the optimal concentration of MO ensures the driving force required for mass transfer between the MO aqueous phase and the solid phase (adsorbent). The highest interaction between MO molecules and the active sites of the AC material provides great removal efficiency at low MO concentrations (Figure 3c). In addition, lower removal efficiency at high MO concentrations could be explained based on the saturation of adsorbent active sites. High MO concentrations cause limited adsorption of the active sites or else increased repulsive electrostatic force between the MO molecules and the adsorbent surface [43,44].

The absorption capacity increased when the initial concentration increased, but the removal efficiencies and the distribution coefficient decrease with the increase in the initial concentration of the MO (Figure 4). The obtained data demonstrate that AC has a limited number of active sites on the specific surface, and with the increase in MO concentration, they are occupied up to maximum capacity. The lack of free active sites on the surface of the AC prevents the removal of MO at high concentrations from aqueous solutions.

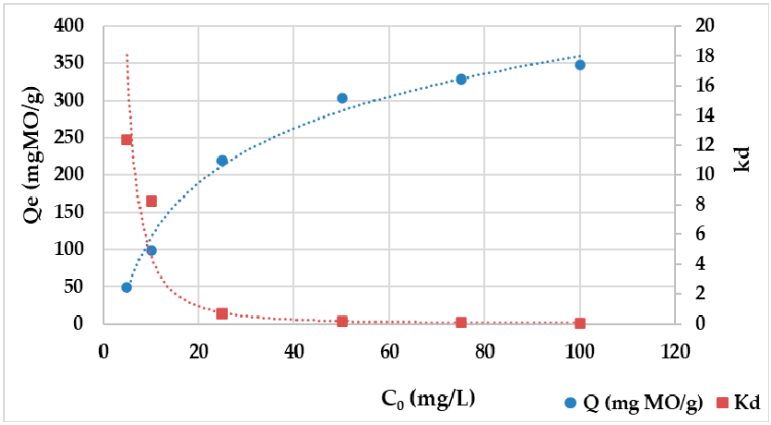

Figure 4. Graphical representation of AC adsorption capacity and distribution coefficient versus the MO initial concentration (adsorbent dose = 0.005 g, MO volume = 50 mL, pH = 3, T = 25 °C).

pH is a key parameter for MO adsorption, and it influences the interactions between the adsorbent material and the organic pollutant. The pH of the solution affects both the surface charge of AC and the ionization of MO molecules. Moreover, π-π and n-π interaction, hydrogen bonds, and hydrophobic interaction could also affect the adsorption process in aqueous solutions [41,45,46]. The removal efficiencies of the MO dye on the AC with pHs ranging between 3 and 11 are shown in Figure 3d. The highest removal efficiency of MO was achieved at pH 3 (namely, 97.8%), and this drastically decreased with the increase in the pH to 42% at pH = 11. This may be due to the change of protons from the available functional groups (transfer or removal) of the adsorbent at different pH values of the aqueous solution, and may also be due to the anionic nature of the MO dye [47].

The pH drift method was used to establish the pH_{pzc}. The determined value of pH_{pzc} was 8.1 (the point where the curve pH_{final} vs. $pH_{initial}$ cross the line $pH_{initial} = pH_{final}$). The zeta potential ($pH_{pzc}$) of AC is dependent on the pH of the aqueous solution (Figure 5). Thus, $pH < pH_{pzc}$ suggests that the AC surface has a net positive charge, while $pH > pH_{pzc}$ suggests that the AC surface has a net negative charge [48,49].

The interaction between the negatively charged MO molecules and the positively charged functional groups of the adsorbent material is due to the electrostatic force of interaction and hydrogen bonds, which is why the predominant interaction between the adsorbate and the adsorbent was observed at low pH values. The good interaction between MO molecules and the surface of AC was transposed in high MO removal efficiency

at lower pH values. The sorption mechanism in acidic medium could be expressed as $AC + H^+ \rightarrow ACH^+ / ACH^+ + MO^- \rightarrow ACH^+ \ldots MO^-$, where MO^- in the acidic medium, and which has the following chemical formula:

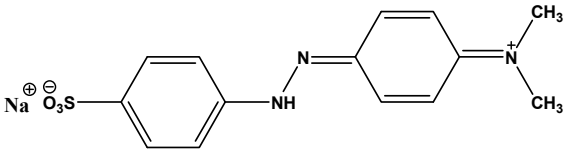

The removal efficiency of MO by adsorption on AC was 97.8% at pH = 3. So, the optimal pH value was 3, and this was used in further experimental studies.

Evaluating the effect of all four of the operational parameters that were tested (adsorbent dosage, interaction time, MO concentration, and pH), the pH proved to be the most important factor affecting the adsorption effect of MO on the activated carbon.

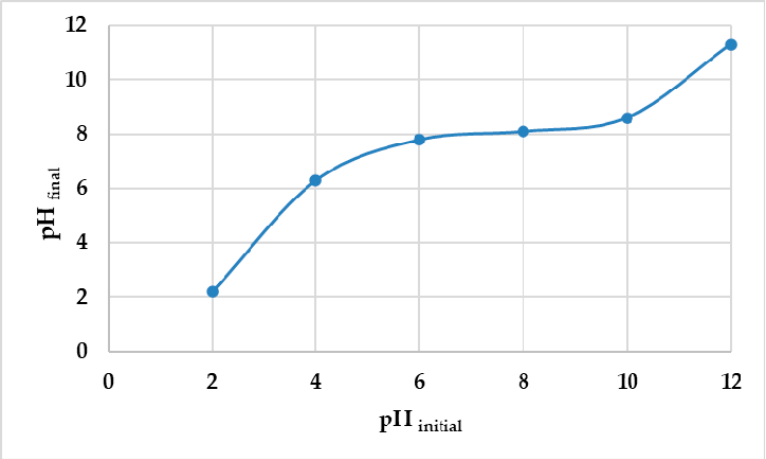

Figure 5. pHpzc of the AC, determined by the pH drift method.

3.3. Isothermal Models

An equilibrium study was performed to examine the adsorption mechanisms occurring between the MO and the adsorbent material interaction using the isothermal adsorption model (Figure 6). Adsorption isotherms provide important information about the adsorption capacity of the adsorbent [35,50]. In this paper, Freundlich and Langmuir isotherm models were used to evaluate the equilibrium data for MO adsorption on AC.

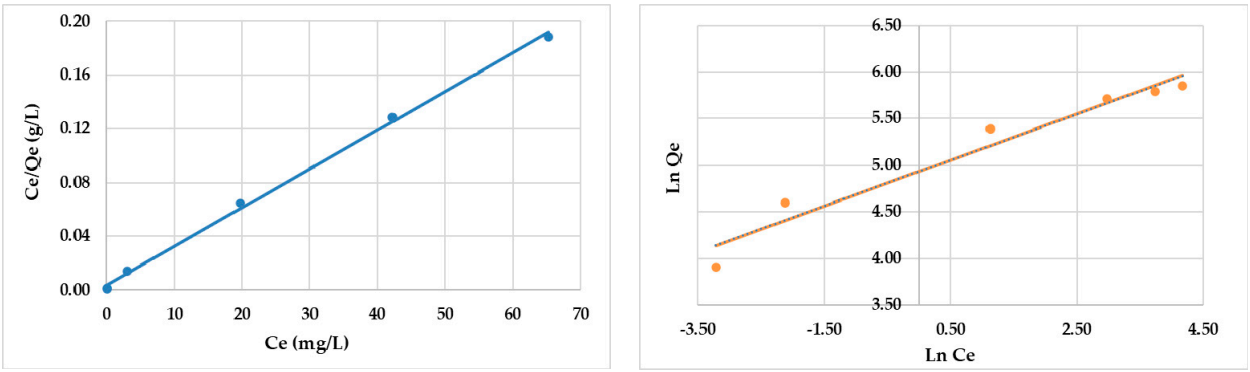

(**a**) (**b**)

Figure 6. Adsorption isotherm of MO on AC: (**a**) Langmuir, and (**b**) Freundlich (adsorbent dose = 0.005 g, MO volume = 50 mL, pH = 3, T = 25 °C).

According to the Langmuir isotherm model, adsorption takes place in a monolayer, the adsorbent molecules being uniformly distributed on the AC surface [51]. In addition, the model assumes that once an adsorbent molecule occupies a free active site, it will no longer be able to adsorb another molecule. The adsorbate occupies all free active sites of the adsorbent material using an equal quantity of energy [52]. The Freundlich adsorption isotherm model is used to describe multilayer adsorption on an adsorbent material with a heterogeneous surface. In this model, the enthalpies and affinities between adsorbent and adsorbate show an unstable distribution [53].

The results obtained were evaluated by the coefficient R^2 derived from the linear regressions of the two isothermal models:

The results summarized in Table 1 demonstrate that the Langmuir isotherm best describes the equilibrium data, the correlation coefficient being 0.9981. This indicates that the adsorption of MO on the AC surface is uniform, and that the monolayer occupation of the free active sites on the surface of the adsorbent material is dominant [52,54]. In addition, the value of the separation factor (RL) was 0.71. This value is situated between $0 < RL < 1$, which demonstrates that MO adsorption on AC can be considered favorable [55,56]. The maximum adsorption capacity determined according to the Langmuir isotherm model was 129.3 mg/g. Similar results were also reported in studies that involved the adsorption of dyes on activated carbon obtained from different materials [33–36,56].

Table 1. Adsorption isotherms parameters.

Adsorbent	Langmuir				Freundlich			
	Q_{max} (mg/g)	K_L (L/mg)	R^2	SD	K_F (mg/g)	n	R^2	SD
AC	129.3 ± 4.13	0.0833 ± 0.003	0.9981	0.322	140 ± 3.22	4.05	0.9554	0.262

3.4. Kinetic Studies

The first-order and pseudo-second order models were used to examine the adsorption mechanisms of MO dye on AC adsorbent. The kinetic parameters for both kinetic models are summarized in Table 2. According to Figure 7, the correlation coefficient (R^2) for the pseudo-second kinetic order graphical representation was 0.9992, which was higher than that obtained for the pseudo-first order kinetic model. Moreover, experimental data obtained for the pseudo-second order kinetic sustained a good accordance with the experimental values of the adsorption capacity at equilibrium (Q_e) with the calculated one. Consequently, the results demonstrated that the adsorption of MO on AC followed the pseudo-second order kinetic model. Thus, the pseudo-second order model assumes that the border surface resistance was not the rate-limiting stage, meaning that the adsorption process consists of two steps: a fast initial one followed by a lent second stage that is restricted by the diffusion of organic dye molecules into the smaller pores, which indicates that the rate of adsorption is proportional to the square of the remaining number of unoccupied adsorption sites [57].

The disadvantages of pseudo-first-order and pseudo-second-order models is that they do not give information about the diffusion mechanism. It is known that film diffusion and intra-particle diffusion are the two mechanisms that control the adsorption process. Thus, one of them is the rate restrictive step [58,59]. For the current case, the adsorption process involved three steps (Figure 8). The intra-particle diffusion model should be a linear regression between qt and $t^{1/2}$, with slope = kid and intercept = C_{id}. If the straight line crosses the origin, the intra-particle diffusion represents the only rate-controlling step. The multi-linear curves exhibited in the current study signify that the adsorption process was described by two or more stages. The first stage **(1)** was a sharp one, and constituted the bulk transfer of MO dye from the aqueous solution. The slow diffusion of MO molecules into the left-out active sites of the AC adsorbent was described by the second stage **(2)**, while the third stage **(3)** represented the equilibrium step.

Table 2. Kinetics parameters for pseudo-first order, pseudo-second order, and intra-particle diffusion.

Pseudo-first-order kinetics	k_1 (min^{-1})	-0.006 ± 0.03
	R^2	0.9564
	Qe (exp) (mg/g)	44.95 ± 1.61
	SD	0.353
Pseudo-second-order kinetics	k_2 (g/mg × min)	46 ± 1.62
	R^2	0.9992
	Q_e (exp) (mg/g)	100 ± 2.83
	SD	0.294
Intra-particle diffusion	K_{id} (g/mg × min)	14.73 ± 0.58
	C_{id}	34.3 ± 1.26
	R^2	0.6855
	SD	0.378

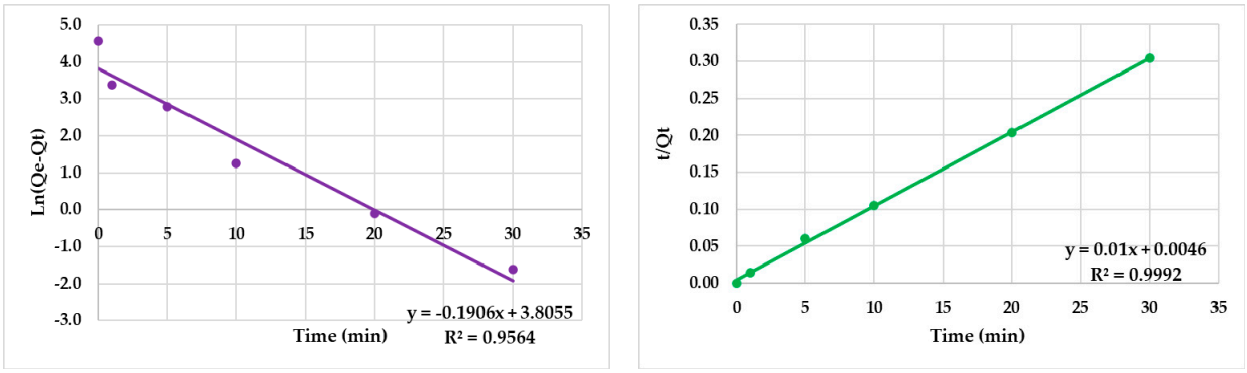

(**a**) (**b**)

Figure 7. Kinetic plots obtained for MO adsorption on AC: (**a**) pseudo-first order, and (**b**) pseudo-second order kinetics.

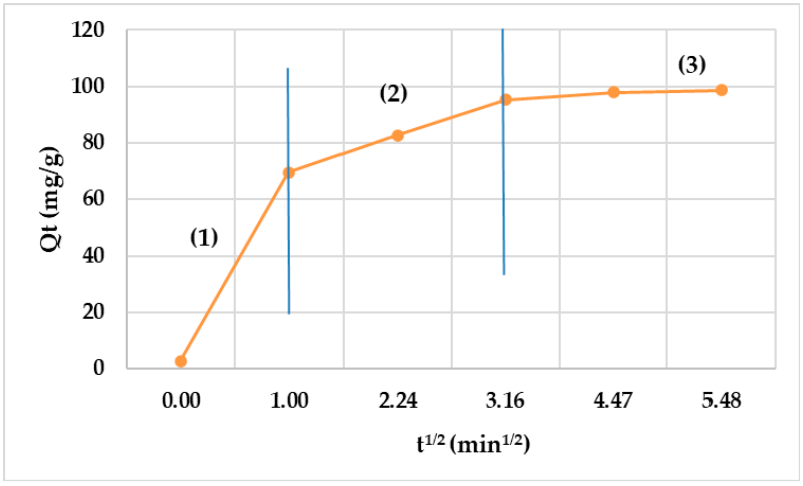

Figure 8. Intra-particle diffusion plot for adsorption of MO dye on AC adsorbent, where (1), (2) and (3) represent the three stages of the adsorption process.

3.5. Thermodynamic Study

Thermodynamic parameters provide insights into the energetics and the feasibility of the adsorption as well as the nature of the interaction between the adsorbent and the adsorbate. The Van't Hoff equation was used to determine the thermodynamic parameters at temperatures that ranged between 25 and 50 °C. The results are provided in Table 3.

Table 3. Thermodynamic parameters for the MO adsorption process.

T (K)	SD	K_L (L/mg)	$K_L^\circ \times 10^5$ (Dimensionless)	Ln K_L°	ΔG° (KJ/mol)	ΔH° (KJ/mol)	ΔS° (J/mol)
298	0.197	0.08 ± 0.003	0.27 ± 0.01	10.21 ± 0.43	−32.87 ± 1.37	−14.94 ± 2.45	60.16 ± 1.55
303	0.225	0.13 ± 0.005	0.41 ± 0.02	10.62 ± 0.45	−33.17 ± 1.40		
308	0.266	0.34 ± 0.02	1.13 ± 0.05	11.63 ± 0.51	−33.47 ± 1.46		
313	0.301	0.72 ± 0.03	2.35 ± 0.09	12.37 ± 0.51	−33.77 ± 1.40		
318	0.358	1.62 ± 0.06	5.31 ± 0.21	13.18 ± 0.52	−34.07 ± 1.35		
323	0.432	3.55 ± 0.13	11.61 ± 0.44	13.97 ± 0.53	−34.38 ± 1.30		

The results revealed negative values for ΔG°, which indicate that the adsorption process of MO dye onto AC material occurred spontaneously, without the need for an external energy source. The negative value determined for ΔH° suggests an exothermic adsorption process [60]. The magnitude of the $\Delta H\circ$ value between −2.1 and −20.9 kJ/mol indicates physical adsorption of MO on the AC material [61]. For ΔS°, positive value was obtained, and this data indicates structural changes on the adsorbent surface as well as random modifications at the solid/liquid interface throughout the adsorption process, which are due to the replacement of the adsorbed water molecules by the MO molecules [26].

In conclusion, the adsorption process of MO dye on to the commercially activated carbon is a spontaneous and exothermic one. The low heat necessary for MO adsorption on the AC material indicates that physical adsorption rather than chemisorption is predominant in this case.

3.6. Application for Real Wastewater Samples

Five wastewater samples collected from different sources were used to evaluate the applicability of the optimized method. AC adsorbent material was used to remove MO from real wastewater samples. Since the samples did not have a quantifiable dye content, they were enriched so that after the controlled contamination, the wastewater samples had an MO dye content of 20 mg/L. Prior to controlled contamination, all of the samples were filtrated on 0.45 µm filters to remove any suspended particles. The results summarized in Table 4 show that the commercial AC was able to remove up to 96.7% of the MO concentration of the wastewater samples.

Table 4. Application of AC on the MO removal from wastewater samples.

Wastewater Samples	Final Conc (mg/L)	Removal (%)
S1	1.22 ± 0.066	93.9
S2	0.87 ± 0.054	95.7
S3	1.47 ± 0.061	92.7
S4	2.03 ± 0.095	89.9
S5	0.66 ± 0.040	96.7

3.7. Desorption and Reusability

Regeneration of the adsorbent material is an important step when the practical and economic viability of the process are under discussion. For experiments with MO-loaded AC for desorption study, the used AC was isolated and washed with ethanol and ultra-purified water a couple of times and then dried for 24 h at 100 °C. The dried AC was reused for batch experiments of MO removal at optimized conditions. The obtained data revealed a decrease of the AC adsorption capacity during the five cycles to 70.3% from 97.8% (Figure 9). In addition, the desorption percentage decreased with the number of regeneration cycles increasing: it was 91.7% after the first cycle, and dropped to 70.3% after the fifth cycle. Thus, we can conclude that the commercial AC that we used can be

successfully used for up to five cycles. Ethanol and water were used in similar studies to recover MO dye from longan seed-derived activated carbon [33].

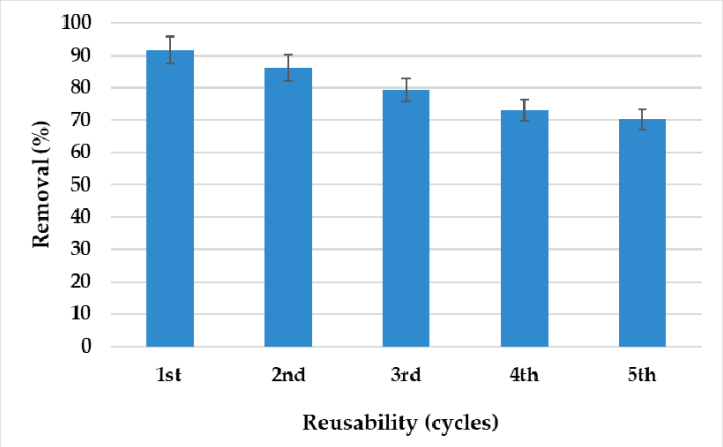

Figure 9. Regeneration capabilities of AC material.

3.8. Adsorption Capabilities of the Commercial AC Material for Other Organic Compounds Removal

The same commercial activated carbon was used as the adsorbent material for treatment wastewater containing nonsteroidal anti-inflammatory drugs, namely, ibuprofen, ac-etaminophen, diclofenac, and ketoprofen [37]. The adsorption studies were conducted using volumes of 50 mL of pharmaceutical compounds at different concentrations (1, 5, and 10 mg/L), and they tested different adsorbent dosages of 0.1, 0.5, and 1 g at two pH values (4 and 6). The organic compounds were quantified using the HPLC technique. The results regarding the optimal adsorption conditions are presented in Table 5.

Table 5. Optimal adsorption condition for anti-inflammatory drugs removal from wastewater using the commercial AC material.

Pharmaceutical Compounds	Adsorbent Dosage (g)	Conc (mg/L)	Solution pH (pH Units)	Removal Efficiencies (%)	Q_{max} (mg/g)
Ibuprofen	1	1	6	96	0.70
Acetaminophen				98	0.64
Diclofenac				92	0.85
Ketoprofen				88	0.66

The highest removal efficiencies were obtained for the lowest concentration tested, and they decreased when the concentration increased (1 to 10 mg/L). The adsorption process of the anti-inflammatory drugs on the activated carbon material at equilibrium were better described by the Langmuir isothermal model, although the date revealed high removal efficiencies, and a high amount of adsorbent material was used (1 g). The maximum adsorption capacities were much lower than the those obtained for the MO dye (in this study). The desorption studies were performed using different concentrations of HCl, and this proved that the desorption process depends on the dissociation constant and the solubility of the anti-inflammatory drugs, with desorption yields of 87.8% for ketoprofen, 80.2% for diclofenac, 73.5% for acetaminophen, and 69.7% for ibuprofen. The data have shown that the AC that was tested in this study could be a feasible adsorbent material for removing the target pharmaceutical compounds from wastewater.

3.9. Comparison with Other Adsorbents

Table 6 summarizes MO removal by different types of commercial activated carbon and different precursors used for activated carbon synthesis. The data reported in the literature

show that both commercial and agricultural precursor-based activated carbons have a high removal capacity (between 48.5% and 100%) of MO from aqueous solutions. Table 6 also provides the reported values for the maximum adsorption capacities in the literature, which range from 10.29 up to 3000 mg/g. Therefore, the commercial AC adsorbent material can be comparable to the specialized literature, reaching a maximum removal of up to 97.8% under the optimal conditions established.

Table 6. Summary of the adsorption of dyes by activated carbon sorbents.

Source of Activated Carbon	Adsorption Capacity (mg/g)	Removal Efficiency (%Re)	References
Dates pits	434	-	[62]
Commercial activated carbon	113.6	90	[63]
Prosopis juliflora bark	10.29	>90	[34]
orange/citrus peels-activated carbon	33	98.0	[35]
Populous leaves charcoal	90.4	-	[36]
Longan seed- activated carbon	464.6	95.8	[33]
Popcorn—activated carbon	969	48.5	[64]
waste tire rubber—activated carbon	588	80.0	[65]
Coconut shell—activated carbon	3000	100	[66]
Activated carbon	78.7	67	[67]
SBA-15	294.1	-	[68]
Coffee grounds	558	-	[69]
Commercial activated carbon	129.3	97.8	This work

The attendance of various adsorbents used by scientists in recent last years for the removal of MO from aqueous solutions are composite, biosorbents, nanoparticles, clays and minerals, biochar, polymers and resins, and activated carbon (Figure 10) [7]. The most oft-used type of adsorbents were the composite ones (42.9%), probably due to their recognized adsorption capacity, and this is a product of the individual materials that are used to create the composite (Figure 10a). Other types of adsorbent materials used are nanoparticles, and the main reason for this is their popularity due to their very small size with a large surface area, which generates a high adsorption capacity. Clays and minerals represent the third group of adsorbent materials used to remove MO dye from aqueous solutions, and this group of materials possesses the ability to adsorb water in their intermediate sites and their large surface area. However, it has been scientifically proven that activated carbon has the highest absorption capacities, with values > 1000 mg/g (Figure 10b) [7].

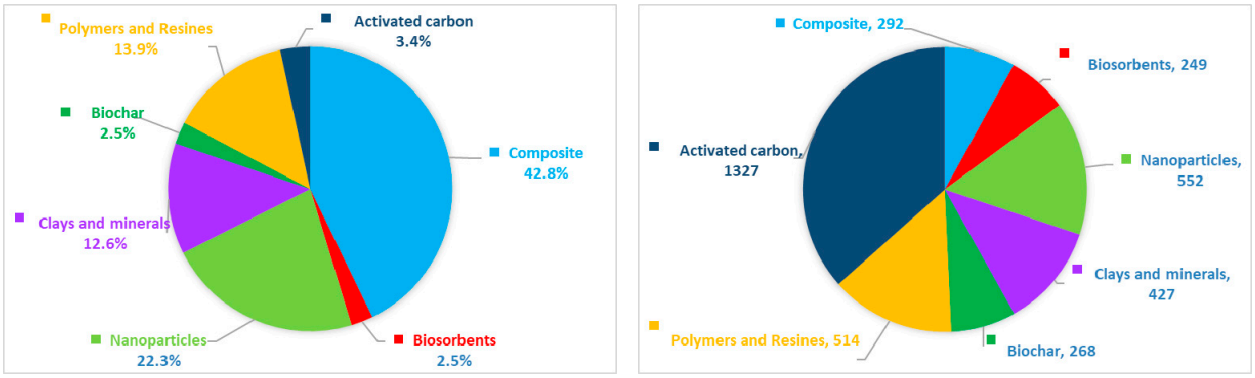

(**a**) (**b**)

Figure 10. (**a**) Frequency of the different types of adsorbents used for MO removal between 2016 and 2021. (**b**) Maximum adsorption capacities for different types of adsorbent materials.

4. Conclusions and Future Work

In this study, the removal of methyl orange dye from aqueous solutions was performed and studied using activated carbon as an adsorbent material. The optimal conditions of the studied remediation process were determined through experiments in which four operational parameters were varied: dosage effect (0.001–0.010 g AC), interaction time (1–120 min), MO concentration (5–100 mg/L MO), and pH (3–11). pH and adsorbent dosage proved to be the most influential parameters for the adsorption of MO. The results revealed an optimal pH value of 3 and an optimal contact time of 30 min for the removal of methyl orange from aqueous solutions by adsorption on activated carbon.

The maximum amount of methyl orange adsorbed on activated carbon was found to be 129.8 mg/g activated carbon, with a maximum removal of 97.8%. The study of the adsorption isotherms shows that the Langmuir isotherm describes the MO adsorption equilibrium behavior, with adsorption of the MO on the AC surface being uniform, and the monolayer occupation of the free active sites on the surface of the adsorbent material is dominant. The kinetic study showed that the adsorption of MO on AC followed the pseudo-second-order kinetic model, which assumes that the adsorption process is based on chemical interaction, providing that the kinetic experiment is initially carried out under conditions of an excess of MO or AC. The negative values determined for the ΔG° parameter demonstrated that the adsorption process involved physical interaction between MO molecules and AC surface sites, while the negative MO adsorption enthalpy (ΔH°) values indicated that the adsorption process was exothermic. The results obtained in this study show that AC could be a possible adsorbent for the MO adsorption process, and that it could be used to successfully remove this dye from wastewater samples.

In future work, we propose to study the adsorption process of other anionic and cationic synthetic dyes using commercial activated carbon, as well as to study the competition between organic molecules to occupy the free active sites of the adsorbent material. In addition, we propose the application of these experimental studies both in the treatment of wastewater through laboratory studies and their extension to obtain basic engineering results for field operation. These studies involve the study of continuous adsorption using fixed-bed columns based on commercial activated carbon. Data on the use of this technology have been previously reported, and have been used to remove various organic molecules, including dyes, using nanocomposite material [70,71]. These studies have demonstrated that the fix-bed column provides a high absorption capacity, resulting in high-quality wastewater.

Author Contributions: Conceptualization, V.I.I. and F.L.C.; data curation, G.V.S., C.D., A.T. and N.V.; formal analysis: G.V.S., F.L.C., A.T. and I.I.; writing—original draft preparation, G.V.S., F.L.C., I.C. and M.N.; writing—review and editing, F.L.C., V.I.I., C.D., I.C., I.I. and M.N.; funding acquisition, I.C., C.D. and M.N. All authors have read and agreed to the published version of the manuscript.

Funding: This research was funded by the Ministry of Research, Innovation, and Digitization of Romania through the Romanian National Research Program "Nucleu", contract no. 3N/2022, A.A.1/2023, Project code PN 23 22 01 01.

Institutional Review Board Statement: Not applicable.

Informed Consent Statement: Not applicable.

Data Availability Statement: Not applicable.

Acknowledgments: The authors acknowledge the financial support offered by the Ministry of Research, Innovation, and Digitization of Romania through the Romanian National Research Program "Nucleu", contract no. 3N/2022, A.A.1/2023, Project code PN 23 22 01 01.

Conflicts of Interest: The authors declare no conflict of interest.

References

1. Al-Tohamy, R.; Ali, S.S.; Li, F.; Okasha, K.M.; Mahmoud, Y.A.-G.; Elsamahy, T.; Jiao, H.; Fu, Y.; Sun, J. A critical review on the treatment of dye-containing wastewater: Ecotoxicological and health concerns of textile dyes and possible remediation approaches for environmental safety. *Ecotoxicol. Environ. Saf.* **2022**, *231*, 1131. [CrossRef]
2. Lellis, B.; Fávaro-Polonio, C.Z.; Pamphile, J.A.; Polonio, J.C. Effects of textile dyes on health and the environment and bioremediation potential of living organisms. *Biotechnol. Res. Innov.* **2019**, *3*, 275–290. [CrossRef]
3. Tomar, T.; Kahandawala, N.; Kaur, J.; Thounaojam, L.; Choudhary, I.; Bera, S. Bioremediation of synthetic dyes from wastewater by using microbial nanocomposites: An emerging field for water pollution management. *Biocatal. Agric. Biotechnol.* **2023**, *51*, 102767. [CrossRef]
4. Garcia, V.S.G.; de Freitas Tallarico, L.; Rosa, J.M.; Suzuki, C.F.; Roubicek, D.A.; Nakano, E.; Borrely, S.I. Multiple adverse effects of textile effluents and reactive Red 239 dye to aquatic organisms. *Environ. Sci. Pollut. Res.* **2021**, *28*, 63202–63214. [CrossRef]
5. Tkaczyk, A.; Mitrowska, K.; Posyniak, A. Synthetic organic dyes as contaminants of the aquatic environment and their implications for ecosystems: A review. *Sci. Total Environ.* **2020**, *717*, 137222. [CrossRef]
6. Mabuza, L.; Sonnenberg, N.; Marx-Pienaar, N. Natural versus synthetic dyes: Consumers' understanding of apparel coloration and their willingness to adopt sustainable alternatives. *Resour. Conserv. Recycl. Adv.* **2023**, *18*, 200146. [CrossRef]
7. Iwuozor, K.O.; Ighalo, J.O.; Emenike, E.C.; Ogunfowora, L.A.; Igwegbe, C.A. Adsorption of methyl orange: A review on adsorbent performance. *Curr. Res. Green Sustain. Chem.* **2021**, *4*, 100179. [CrossRef]
8. Sugai, D.Y.; Benincá, C.; Zanoelo, E.F. Electrogenerated iron-based adsorbents: A case study of an azo dye removal viewed from a fundamental physico-chemical perspective. *J. Chem. Eng.* **2023**, *454*, 140129. [CrossRef]
9. Chen, C.; Cao, Y.; Ali, A.; Toufouki, S.; Yao, S. How to apply terpenoid-based deep eutectic solvents for removal of antibiotics and dyes from water: Theoretical prediction, experimental validation and quantum chemical evaluation. *Environ. Res.* **2023**, *231*, 116180. [CrossRef]
10. Gita, S.; Shukla, S.P.; Deshmukhe, G.; Singh, A.R.; Choudhury, T.G. Adsorption linked fungal degradation process for complete removal of Lanasyn olive dye using chemically valorized sugarcane bagasse. *Waste Manag. Bull.* **2023**, *1*, 29–38. [CrossRef]
11. Chu, Y.; Zhu, S.; Wang, F.; Lei, W.; Xia, M.; Liao, C. Tyrosine-Immobilized Mont-morillonite: An Efficient Adsorbent for Removal of Pb^{2+} and Cu^{2+} from Aqueous Solution. *J. Chem. Eng. Data* **2019**, *64*, 3535–3546. [CrossRef]
12. Zhu, S.; Chen, Y.; Khan, M.A.; Xu, H.; Wang, F.; Xia, M. Interfaces, In-Depth Study of Heavy Metal Removal by an Etidronic Acid-Functionalized Layered Double Hydroxide. *Appl. Mater.* **2022**, *14*, 7450–7463. [CrossRef]
13. Amjad, S.; Shaukat, S.; Rahman, H.M.A.U.; Usman, M.; Farooqi, Z.H.; Nazar, M.F. Application of anionic-nonionic mixed micellar system for solubilization of methylene blue dye. *J. Mol. Liq.* **2023**, *369*, 120958. [CrossRef]
14. Yusaf, A.; Usman, M.; Siddiq, M.; Bakhtiar, M.; Mansha, A.; Shaukat, S.; Rehman, H.F. Mixed micellar solubilization of Naphthol Green B followed by its removal from synthetic effluent by micellar-enhanced ultrafiltration under optimized conditions. *Molecules* **2022**, *27*, 6436. [CrossRef] [PubMed]
15. Rehman, A.; Nisa, M.U.; Usman, M.; Ahmad, Z.; Bokhari, T.H.; Rahman, H.M.A.U.; Rasheed, A.; Kiran, L. Application of cationic-nonionic surfactant based nanostructured dye carriers: Mixed micellar solubilization. *J. Mol. Liq.* **2021**, *326*, 115345. [CrossRef]
16. Debnath, S.; Das, R. Strong adsorption of CV dye by Ni ferrite nanoparticles for waste water purification: Fits well the pseudo second order kinetic and Freundlich isotherm model. *Ceram. Int.* **2023**, *49*, 16199–16215. [CrossRef]
17. He, S.; Li, J.; Cao, X.; Xie, F.; Yang, H.; Wang, C.; Bittencourt, C.; Li, W. Regenerated cellulose/chitosan composite aerogel with highly efficient adsorption for anionic dyes. *Int. J. Biol. Macromol.* **2023**, *244*, 125067. [CrossRef]
18. Chang, S.; Simeng, Y.; Henglong, T.; Shihao, F.; Zhu, L. Adsorption properties and interactions analysis of cyclodextrin-based polymer networks towards organic dyes. *Carbohydr. Polym. Technol. Appl.* **2023**, *5*, 100317. [CrossRef]
19. Elabboudi, M.; Bensalah, J.; Amri, A.E.; Azzouzi, N.E.; Srhir, B.; Lebkiri, A.; Zarrouk, A.; Rifi, E.H. Adsorption performance and mechanism of anionic MO dye by the adsorbent polymeric Amberlite®IRA-410 resin from environment wastewater: Equilibrium kinetic and thermodynamic studies. *J. Mol. Struct.* **2023**, *1277*, 134789. [CrossRef]
20. Thamer, B.M.; Shaker, A.A.; Hameed, M.M.A.; Al-Enizi, A.M. Highly selective and reusable nanoadsorbent based on expansive clay-incorporated polymeric nanofibers for cationic dye adsorption in single and binary systems. *J. Water Process. Eng.* **2023**, *54*, 103918. [CrossRef]
21. El-taweel, R.M.; Mohamed, N.; Alrefaey, K.A.; Husien, S.; Abdel-Aziz, A.B.; Salim, A.I.; Mostafa, N.G.; Said, L.A.; Fahim, I.S.; Radwan, A.G. A review of coagulation explaining its definition, mechanism, coagulant types, and optimization models; RSM, and ANN. *Curr. Opin. Green Sustain. Chem.* **2023**, *6*, 100358. [CrossRef]
22. Ma, H.; Zhou, W.; Xu, X.; Zhu, X.; Wang, L.; Shi, X.; Jiang, M.; Li, C.; Li, T. Characterizing the removal of Pb^{2+} and Zn^{2+} from an acidic smelting wastewater using electrocatalytic internal Fe0/C micro-electrolysis. *Sep. Purif. Technol.* **2023**, *317*, 123874. [CrossRef]
23. Pan, Z.F.; An, L. Removal of Heavy Metal from Wastewater Using Ion Exchange Membranes. In *Applications of Ion Exchange Materials in the Environment*; Ahamed, M.I., Asiri, A., Eds.; Springer: Cham, Switzerland, 2019. [CrossRef]
24. Selvasembian, R.; Gwenzi, W.; Chaukura, N.; Mthembu, S. Recent advances in the polyurethane-based adsorbents for the decontamination of hazardous wastewater pollutants. *J. Hazard. Mat.* **2021**, *417*, 125960. [CrossRef]

25. Adithya, G.T.; Rangabhashiyam, S.; Sivasankari, C. Lanthanum-iron binary oxide nanoparticles: As cost-effective fluoride adsorbent and oxygen gas sensor. *Microchem. J.* **2019**, *148*, 364–373. [CrossRef]
26. Imessaoudene, A.; Cheikh, S.; Bollinger, J.-C.; Belkhiri, L.; Tiri, A.; Bouzaza, A.; El Jery, A.; Assadi, A.; Amrane, A.; Mouni, L. Zeolite Waste Characterization and Use as Low-Cost, Ecofriendly, and Sustainable Material for Malachite Green and Methylene Blue Dyes Removal: Box–Behnken Design, Kinetics, and Thermodynamics. *Appl. Sci.* **2022**, *12*, 7587. [CrossRef]
27. Naseem, K.; Farooqi, Z.H.; Begum, R.; Rehman, M.Z.U.; Shahbaz, A.; Farooq, U.; Ali, M.; Rahman, H.M.A.U.; Irfan, A.; Al-Sehemi, A.G. Removal of Cadmium (II) from Aqueous Medium Using Vigna radiata Leave Biomass: Equilibrium Isotherms, Kinetics and Thermodynamics. *Z. Fur Phys. Chem.* **2019**, *233*, 669–690. [CrossRef]
28. Boudechiche, N.; Fares, M.; Ouyahia, S.; Yazid, H.; Trari, M.; Sadaoui, Z. Comparative study on removal of two basic dyes in aqueous medium by adsorption using activated carbon from Ziziphus lotus stones. *Microchem. J.* **2019**, *146*, 1010–1018. [CrossRef]
29. Giannakoudakis, D.A.; Kyzas, G.Z.; Avranas, A.; Lazaridis, N.K. Multi-parametric adsorption effects of the reactive dye removal with commercial activated carbons. *J. Mol. Liq.* **2016**, *213*, 381–389. [CrossRef]
30. Husien, S.; El-taweel, R.M.; Salim, A.I.; Fahim, I.S.; Said, L.A.; Radwan, A.G. Review of activated carbon adsorbent material for textile dyes removal: Preparation, and modelling. *Cur. Res. Green Sustain. Chem.* **2022**, *5*, 100325. [CrossRef]
31. Azari, A.; Nabizadeh, R.; Nasseri, S.; Mahvi, A.H.; Mesdaghinia, A.R. Comprehensive systematic review and meta-analysis of dyes adsorption by carbon-based adsorbent materials: Classification and analysis of last decade studies. *Chemosphere* **2020**, *250*, 126238. [CrossRef] [PubMed]
32. Mammar, A.C.; Mouni, L.; Bollinger, J.-C.; Belkhiri, L.; Bouzaza, A.; Assadi, A.A.; Belkacemi, H. Modeling and optimization of process parameters in elucidating the adsorption mechanism of Gallic acid on activated carbon prepared from date stones. *Sep. Sci. Technol.* **2019**, *55*, 3113–3125. [CrossRef]
33. Hung, N.V.; Nguyet, B.T.M.; Nghi, N.H.; Thanh, N.M.; Quyen, N.D.V.; Nguyen, V.T.; Nhiem, D.N.; Khieu, D.Q. Highly effective adsorption of organic dyes from aqueous solutions on longan seed-derived activated carbon. *Environ. Eng. Res.* **2023**, *28*, 220116. [CrossRef]
34. Kumar, M.; Tamilarasan, R. Modeling of experimental data for the adsorption of methyl orange from aqueous solution using a low cost activated carbon prepared from *Prosopis julifl* ora. *Pol. J. Chem. Technol.* **2013**, *15*, 29–39. [CrossRef]
35. Ramutshatsha-Makhwedzha, D.; Mavhungu, A.; Moropeng, M.L.; Mbaya, R. Activated carbon derived from waste orange and lemon peels for the adsorption of methyl orange and methylene blue dyes from wastewater. *Heliyon* **2022**, *8*, e09930. [CrossRef] [PubMed]
36. Shah, S.S.; Sharma, T.; Dar, B.A.; Bamezai, R.K. Adsorptive removal of methyl orange dye from aqueous solution using populous leaves: Insights from kinetics, thermodynamics and computational studies. *Environ. Chem. Ecotoxicol.* **2021**, *3*, 172–181. [CrossRef]
37. Pirvu, F.; Covaliu-Mierla, C.I.; Paun, I.; Paraschiv, G.; Iancu, V. Treatment of Wastewater Containing Nonsteroidal Anti-Inflammatory Drugs Using Activated Carbon Material. *Materials* **2022**, *15*, 559. [CrossRef]
38. Zhang, P.K.; Wang, L. Extended Langmuir equation for correlating multilayer adsorption equilibrium data. *Sep. Purif. Technol.* **2010**, *70*, 367–371. [CrossRef]
39. Jeppu, G.P.; Clement, T.P. A modified Langmuir-Freundlich isotherm model for simulating pH-dependent adsorption effects. *J. Contam. Hydrol.* **2012**, *129–130*, 46–53. [CrossRef] [PubMed]
40. Lagergren, B.K.S. Svenska Zur Theorie Der Sogenannten Adsorption Geloster Stofe, Kungliga Svenska Vetenskapsakademiens. *Handlingar* **1989**, *24*, 1–39.
41. Olusegun, S.J.; Mohallem, N.D. Comparative adsorption mechanism of doxycycline and congo red using synthesized kaolinite supported CoFe2O4 nanoparticles. *Environ. Pollut.* **2020**, *260*, 114019. [CrossRef]
42. Esvandi, Z.; Foroutan, R.; Peighambardoust, S.J.; Akbari, A.; Ramavandi, B. Uptake of anionic and cationic dyes from water using natural clay and clay/starch/MnFe2O4 magnetic nanocomposite. *Surf. Interfaces* **2020**, *21*, 100754. [CrossRef]
43. Mahmoudi, E.; Azizkhani, S.; Mohammad, A.W.; Ng, L.Y.; Benamor, A.; Ang, W.L.; Ba-Abbad, M. Simultaneous removal of congo red and cadmium (II) from aqueous solutions using graphene oxide–silica composite as a multifunctional adsorbent. *J. Environ. Sci.* **2020**, *98*, 151–160. [CrossRef]
44. Wang, J.; Zhang, W.; Kang, X.; Zhang, C. Rapid and efficient recovery of silver with nanoscale zerovalent iron supported on high performance activated carbon derived from straw biomass. *Environ. Pollut.* **2019**, *255*, 113043. [CrossRef]
45. Hu, Y.; Guo, T.; Ye, X.; Li, Q.; Guo, M.; Liu, H.; Wu, Z. Dye adsorption by resins: Effect of ionic strength on hydrophobic and electrostatic interactions. *Chem. Eng. J.* **2013**, *228*, 392–397. [CrossRef]
46. Li, Y.; Du, Q.; Liu, T.; Sun, J.; Wang, Y.; Wu, S.; Wang, Z.; Xia, Y.; Xia, L. Methylene blue adsorption on graphene oxide/calcium alginate composites. *Carbohydr. Polym.* **2013**, *95*, 501–507. [CrossRef]
47. Kanani-jazi, M.H.; Akbari, S. Journal of Environmental Chemical Engineering Amino-dendritic and carboxyl functionalized halloysite nanotubes for highly efficient removal of cationic and anionic dyes: Kinetic, isotherm, and thermodynamic studies. *J. Environ. Chem. Eng.* **2021**, *9*, 105214. [CrossRef]
48. Tay, W.Y.; Ng, L.Y.; Ng, C.Y.; Sim, L.C. Removal of Methyl Red using Adsorbent Produced from Empty Fruit Bunches by Taguchi Approach. *IOP Conf. Ser. Earth Environ. Sci.* **2021**, *945*, 012014. [CrossRef]
49. Dai, M. The Effect of Zeta Potential of Activate Carbon on the Adsorption of Dyes from Aqueous Solution. *J. Colloid Interface Sci.* **1994**, *164*, 223–228. [CrossRef]

50. Aftab, R.A.; Zaidi, S.; Khan, A.A.P.; Usman, M.A.; Khan, A.Y.; Chani, M.T.S.; Asiri, A.M. Removal of congo red from water by adsorption onto activated carbon derived from waste black cardamom peels and machine learning modeling. *Alex. Eng. J.* **2023**, *71*, 355–369. [CrossRef]
51. Bhomick, C.; Supong, A.; Baruah, M.; Pongener, C.; Sinha, D. Pine Cone biomass as an efficient precursor for the synthesis of activated biocarbon for adsorption of anionic dye from aqueous solution: Isotherm, kinetic, thermodynamic and regeneration studies. *Sustain. Chem. Pharm.* **2018**, *10*, 41–49. [CrossRef]
52. Langmuir, I. The adsorption of gases on plane surfaces of glass, mica and platinum. *J. Am. Chem. Soc.* **1918**, *40*, 1361–1403. [CrossRef]
53. Freundlich, H.M.F. Over the adsorption in solution. *J. Phys. Chem.* **1906**, *57*, 385–471. [CrossRef]
54. Ahmad, M.A.; Puad, N.A.A.; Bello, O.S. Kinetic, equilibrium and thermodynamic studies of synthetic dye removal using pomegranate peel activated carbon prepared by microwave-induced KOH activation. *Water Res. Ind.* **2014**, *6*, 18–35. [CrossRef]
55. Mahamad, M.N.; Zaini, M.A.A.; Zakaria, Z.A. Preparation and characterization of activated carbon from pineapple waste biomass for dye removal. *Int. Biodeterior. Biodegrad.* **2015**, *102*, 274–280. [CrossRef]
56. Nizam, N.U.M.; Hanafiah, M.M.; Mahmoudi, E.; Halim, A.A.; Mohammad, A.W. The removal of anionic and cationic dyes from an aqueous solution using biomass-based activated carbon. *Sci. Rep.* **2021**, *11*, 8623. [CrossRef]
57. Foo, K.Y.; Hameed, B.H. Microwave-assisted preparation and adsorption performance of activated carbon from biodiesel industry solid reside: Influence of operational parameters. *Bioresour. Technol.* **2012**, *103*, 398–404. [CrossRef] [PubMed]
58. Bouaziz, F.; Koubaa, M.; Kallel, F.; Chaari, F.; Driss, D.; Ghorbel, R.E.; Chaabouni, S.E. Efficiency of almond gum as a low cost adsorbent for methylene blue dye removal from aqueous solutions. *Ind. Crop Prod.* **2015**, *74*, 903–911. [CrossRef]
59. Qiu, H.; Lv, L.; Pan, B.; Zhang, Q.; Zhang, W.; Zhang, Q. Critical review in adsorption kinetic models. *J. Zhejiang Univ.—Sci. A* **2009**, *10*, 716–724. [CrossRef]
60. Foroutan, R.; Peighambardoust, S.J.; Peighambardoust, S.H.; Pateiro, M.; Lorenzo, J.M. Adsorption of Crystal Violet Dye Using Activated Carbon of LemonWood and Activated Carbon/Fe_3O_4 Magnetic Nanocomposite from Aqueous Solutions: A Kinetic, Equilibrium and Thermodynamic Study. *Molecules* **2021**, *26*, 2241. [CrossRef]
61. Humpola, P.D.; Odetti, H.S.; Fertitta, A.E.; Vicente, J.L. Thermodynamic analysis of adsorption models of phenol in liquid phase on different activated carbons. *J. Chil. Chem. Soc.* **2013**, *58*, 1541–1544. [CrossRef]
62. Mahmoudi, K.; Hosni, K.; Hamdi, N.; Srasra, E. Kinetics and equilibrium studies on removal of methylene blue and methyl orange by adsorption onto activated carbon prepared from date pits-A comparative study. *Korean J. Chem. Eng.* **2015**, *32*, 274–283. [CrossRef]
63. Khattabi, E.H.E.L.; Rachdi, Y.; Bassam, R.; Mourid, E.H.; Naimi, Y.; Alouani, M.E.L.; Belaaouad, S. Enhanced elimination of methyl orange and recycling of an eco-friendly adsorbent activated carbon from aqueous solution. *Russ. J. Phys. Chem. B* **2021**, *15* (Suppl. S2), S149–S159. [CrossRef]
64. Yu, Y.; Qiao, N.; Wang, D.; Zhu, Q.; Fu, F.; Cao, R.; Wang, R.; Liu, W.; Xu, B. Fluffy honeycomb-like activated carbon from popcorn with high surface area and well-developed porosity for ultra-high efficiency adsorption of organic dyes. *Bioresour. Technol.* **2019**, *285*, 121340. [CrossRef]
65. Islam, M.T.; Saenz-Arana, R.; Hernandez, C.; Guinto, T.; Ahsan, M.A.; Bragg, D.T.; Wang, H.; Alvarado-Tenorio, B.; Noveron, J.C. Conversion of waste tire rubber into a high-capacity adsorbent for the removal of methylene blue, methyl orange, and tetracycline from water. *J. Environ. Chem. Eng.* **2018**, *6*, 3070–3082. [CrossRef]
66. Islam, M.S.; Ang, B.C.; Gharehkhani, S.; Afif, A.B.M. Adsorption capability of activated carbon synthesized from coconut shell. *Carbon Lett.* **2016**, *20*, 1–9. [CrossRef]
67. Ahlawat, W.; Kataria, N.; Dilbaghi, N.; Hassan, A.A.; Kumar, S.; Kim, K.H. Carbonaceous nanomaterials as effective and efficient platforms for removal of dyes from aqueous systems. *Environ. Res.* **2020**, *181*, 108904. [CrossRef]
68. Mohammadi, N.; Khani, H.; Gupta, V.K.; Amereh, E.; Agarwal, S. Adsorption process of methyl orange dye onto mesoporous carbon material-kinetic and thermodynamic studies. *J. Colloid Interface Sci.* **2011**, *362*, 457–562. [CrossRef]
69. Rattanapan, S.; Srikram, J.; Kongsune, P. Adsorption of Methyl Orange on Coffee grounds Activated Carbon. *Energy Procedia* **2017**, *138*, 949–954. [CrossRef]
70. Alardhi, S.M.; Albayati, T.M.; Alrubaye, J.M. Adsorption of the methyl green dye pollutant from aqueous solution using mesoporous materials MCM-41 in a fixed-bed column. *Heliyon* **2020**, *6*, e03253. [CrossRef]
71. Ali, M.A.; Mubarak, M.F.; Keshawy, M.; Zayed, M.A.; Ataalla, M. Adsorption of Tartrazine anionic dye by novel fixed bed Core-Shell-polystyrene Divinylbenzene/Magnetite nanocomposite. *Alex. Eng. J.* **2022**, *61*, 1335–1352. [CrossRef]